

DEUTSCHES ELEKTRONEN – SYNCHROTRON

DESY 93-029
March 1993



A Search for Leptoquarks, Leptogluons and Excited Leptons in H1 at HERA

H1 Collaboration

ISSN 0418-9833

NOTKESTRASSE 85 · D - 2000 HAMBURG 52

DESY behält sich alle Rechte für den Fall der Schutzrechtserteilung und für die wirtschaftliche Verwertung der in diesem Bericht enthaltenen Informationen vor.

DESY reserves all rights for commercial use of information included in this report, especially in case of filing application for or grant of patents.

To be sure that your preprints are promptly included in the
HIGH ENERGY PHYSICS INDEX,
send them to (if possible by air mail):

DESY
Bibliothek
Notkestraße 85
W-2000 Hamburg 52
Germany

DESY-IfH
Bibliothek
Platanenallee 6
D-1615 Zeuthen
Germany

- I. Abt⁷, T. Ahmed³, V. Andreev²⁴, B. Andrieu²⁷, R.-D. Appuhn¹¹, M. Arpagaus³⁴, A. Babaev²⁸, H. Bäwolff³³, J. Bán¹⁷, P. Baranov²⁴, E. Barrete²⁸, W. Bartel¹¹, U. Bassler²⁸, H.P. Beck³⁵, H.-J. Behrendt¹¹, A. Belousov²⁴, Ch. Berger¹, H. Bergstein¹, G. Bernard²⁸, R. Bernet³⁴, G. Bertrand, Coremans⁴, M. Besaucon⁹, P. Biddulph²², E. Binder¹¹, A. Bischoff³³, J.C. Bizot²⁸, V. Blobe¹³, K. Borras⁸, P.C. Bosetti², V. Boudry²⁷, C. Bourdarios²⁶, F. Brasse¹¹, U. Braun², W. Braunschweig¹, V. Brisson¹⁹, D. Bruncko¹⁷, L. Büngener¹³, J. Bürger¹¹, F.W. Büsser¹³, A. Buntjatian^{11,37}, S. Burke¹⁹, G. Buschhorn²⁵, A.J. Campbell¹⁰, T. Carl²⁵, F. Charles²⁸, D. Clarke⁵, A.B. Clegg¹⁸, M. Colombo⁸, J.A. Coughlan⁵, A. Courau²⁶, Ch. Coutures⁹, G. Cozzika⁹, L. Criegue¹¹, J. Crach²⁷, S. Dagoret²⁸, J.B. Dainton¹⁹, M. Danilov²³, A.W.E. Dann²², W.D. Dau¹⁸, M. David⁹, E. Deffur¹¹, B. Delcourt²⁶, L. Del Buono²⁸, M. Devet²⁶, A. De Roeck¹¹, P. Dingus²⁷, C. Dollfus³⁵, J.D. Dowell³, H.B. Dreis², A. Drescher⁸, J. Duboc²⁸, D. Düllmann¹³, O. Dünger¹³, H. Duhm¹², R. Ebbinghaus⁸, M. Eberle¹², J. Ebert³², T.R. Ebert¹⁹, G. Eckerlin¹¹, V. Efremenko²³, S. Egli³⁸, S. Eicherberger³⁶, R. Eichler³⁴, F. Eisele¹⁴, E. Eisenhandler²⁰, N.N. Ellis³, R.J. Ellison²², E. Elsen¹¹, M. Erdmann¹¹, E. Evrard⁴, L. Favart⁴, A. Fedotov²³, D. Feeken¹³, R. Felst¹¹, J. Feltesse⁹, F.F. Fensome³, J. Ferencei¹¹, F. Ferrarotto³¹, K. Flamm¹¹, W. Flauger^{11,17}, M. Fleischer¹¹, G. Flüge², A. Fomenko²⁴, B. Foninykh²³, M. Forbush⁷, J. Formánek²⁰, J.M. Foster²², G. Franke¹¹, E. Fretwurst¹², P. Fuhrmann¹, E. Gabathuler¹⁹, K. Gardneringer²⁵, J. Garvey³, J. Gayler¹¹, A. Gellrich¹³, M. Genni¹¹, H. Genzel¹, R. Gerhard¹¹, D. Gillespie¹⁹, L. Godfrey⁷, U. Goerlach¹¹, L. Goerlich⁶, M. Goldberg²⁸, A.M. Goodall¹⁹, I. Gorelov²³, P. Goritschev²³, C. Grab³⁴, H. Gräßler², R. Grässler², T. Greenshaw¹⁹, H. Greif²⁵, G. Grindhammer²⁵, C. Gruber¹⁶, J. Haack³³, D. Haidt¹¹, L. Hajduk⁶, O. Hanon²⁸, D. Handschuh¹¹, E.M. Hanlon¹⁸, M. Hapke¹¹, J. Harjes¹¹, R. Haydar²⁶, W.J. Haynes⁵, J. Heatherington²⁰, V. Hedberg²¹, G. Heinzelmann¹³, R.C.W. Henderson¹⁸, H. Henschel³³, R. Herma¹, I. Herynek²⁹, W. Hildesheim²⁸, P. Hill¹¹, C.D. Hilton²², J. Hladký³⁹, K.C. Hoeger²², Ph. Huet⁴, H. Hufnagel⁸, N. Huot²⁸, M. Ibbotson²², H. Itterbeck¹, M.A. Iaboli⁹, A. Jacholkowska²⁸, C. Jacobsson²¹, M. Jaffre²⁶, T. Janssen¹¹, L. Jönsson²¹, K. Johansen¹³, D.P. Johnson⁴, L. Johnson¹⁸, H. Jung², P.J.P. Kalmus²⁰, S. Kaasariani¹¹, R. Kaschowitz², P. Kasselmann¹², U. Kathage¹⁶, H. H. Kaufmann³³, I.R. Kenyon³, S. Kermicâ²⁸, C. Keuker¹, C. Kiesling²⁵, M. Klein³³, C. Kleinwort¹³, G. Kries¹¹, W. Ko⁷, T. Köhler¹, H. Kolamiski⁸, F. Kole⁷, S.D. Kolya²², V. Korbel¹¹, M. Korn⁸, P. Kostka³³, S.K. Kotelnikov²⁴, M.W. Krasný^{6,28}, H. Kreibiel¹¹, D. Krucker², U. Krüger¹¹, J.P. Kubenek²⁵, H. Küster², M. Kuhlens²⁵, T. Kurčák¹⁷, J. Kurzhofer⁸, B. Kuznik³², R. Lander⁷, M.P.J. Landdon²⁰, W. Lange³³, R. Langenkau¹², P. Lanis²⁵, J.F. Laporte⁸, A. Lebedev²⁴, A. Leuschner¹¹, C. Leverenz¹¹, S. Leonian^{11,24}, D. Lewin¹¹, Ch. Ley², A. Lindner⁸, G. Lindström¹², J. Lipinski¹³, P. Loch¹¹, H. Lohmander²¹, G.C. Lopez²⁰, D. Lüters^{35,†}, N. Magnussen³², E. Malinovski²⁴, S. Mani⁷, P. Marago⁴, J. Marks¹⁰, R. Marshall²², J. Martens³², R. Martin¹⁹, H.-U. Martyn¹, J. Martyniak⁶, S. Masson², A. Mavroidis²⁰, S.J. Maxfield¹⁹, S.J. McMahon¹⁹, A. Mehta²², K. Meier¹⁵, D. Mercer²², T. Merz¹¹, C.A. Meyer³⁵, H. Meyer³², J. Meyer¹¹, S. Mikocki^{6,26}, V. Milone³¹, E. Monnier²⁸, F. Moreau²⁷, J. Moreels⁴, J.V. Morris⁵, K. Müller³⁵, P. Murin¹⁷, S.A. Murray²², V. Nagovizin²⁴, B. Naroska¹³, Th. Naumann³³, D. Newton¹⁸, D. Neyret²⁸, H.K. Nguyen²⁸, F. Niebergall¹³, R. Nisius¹, G. Nowak⁶, G.W. Noyes², M. Nyberg²¹, H. Oberlack²⁶, U. Obrock⁸, J.E. Olsom¹¹, S. Orenstein²⁷, F. Ould-Saada¹³, C. Pascaud²⁶, G.D. Patel¹⁹, E. Peppel¹¹, S. Peters²⁶, J.P. Pharabod²⁷, H.T. Phillips³, J.P. Phillips²², Ch. Pichler¹², W. Pilgram², D. Pitzl³⁴, R. Pros¹¹,

G. Rädel¹¹, F. Raupach¹, K. Rauschnabel⁸, P. Reimer²⁹, P. Ribarics²⁵, V. Riech¹², J. Riedberger³⁴, M. Riezz², S.M. Robertson³, P. Rohmann³⁵, R. Roosen⁴, A. Rostovtsev²³, C. Royon⁹, M. Rudowicz²⁵, M. Ruffer¹², S. Rusakov²⁴, K. Rybicki⁶, N. Sahinman², E. Sanchez²⁵, D.P.C. Sankey⁵, M. Savitsky¹¹, P. Schacht²⁵, P. Schleper¹⁴, W. von Schlippe²⁰, C. Schmidt¹¹, D. Schmidt³², W. Schmitz², V. Schröder¹¹, M. Schulz¹¹, A. Schwind³³, W. Scobell¹², U. Seehausen¹³, R. Sell¹¹, M. Seman¹⁷, A. Semenov²³, V. Shekelyan²³, I. Sheviakov²⁴, H. Shooshbari³¹, G. Siegmon¹⁶, U. Sievert¹⁶, Y. Sirois²⁷, I.O. Skillicon¹⁰, P. Smirnov²⁴, J.R. Smith⁷, L. Smolik¹¹, Y. Soloviev²⁴, H. Spitzer¹³, P. Staroba²⁹, M. Steenbock¹³, P. Steffen¹¹, R. Steinberg², B. Stella³¹, K. Stephens²², J. Stier¹¹, U. Stößlein³³, J. Strachota¹¹, U. Straumann³⁵, W. Struzinski², J.P. Sutton³, R.E. Taylor^{36,26}, C. Thiebaux²⁷, G. Thompson²⁰, I. Tichomirov²³, C. Trenkel¹⁶, P. Trnöl³⁵, V. Tchernyshov²³, J. Turnau⁶, J. Tufts¹⁴, L. Urban²⁵, A. Usik²⁴, S. Valkarova³⁰, A. Valkarova³⁰, C. Vallee²⁸, P. Van Esch⁴, A. Vartapetian^{11,37}, Y. Vazdik²⁴, M. Vecko²⁹, P. Verrecchia⁹, R. Vick¹³, G. Villet⁹, E. Vogel¹, K. Wacker⁸, I.W. Walker¹⁸, A. Walther⁸, G. Weber¹³, D. Wegener⁸, A. Wegner¹¹, H. P. Wellisch²⁶, S. Willard⁷, M. Winde³³, G.-G. Winter¹¹, Th. Wolff³⁴, L.A. Womersley¹⁹, A.E. Wright²², N. Wulff¹¹, T.P. Yiou²⁸, J. Žáček³⁰, P. Závada²⁹, C. Zeitnitz¹², H. Ziaeepour²⁶, M. Zimmer¹¹, W. Zimmermann¹¹, and F. Zomer²⁶.

¹ *I. Physikalisches Institut der RWTH, Aachen, Germany^a*

² *III. Physikalisches Institut der RWTH, Aachen, Germany^a*

³ *School of Physics and Space Research, University of Birmingham, Birmingham, UK^b*

⁴ *Inter-University Institute for High Energies ULB-VUB, Brussels, Belgium^c*

⁵ *Rutherford Appleton Laboratory, Chilton, Didcot, UK^d*

⁶ *Institute for Nuclear Physics, Cracow, Poland*

⁷ *Physics Department and IIRPA, University of California, Davis, California, USA^d*

⁸ *Institut für Physik, Universität Dortmund, Dortmund, Germany^a*

⁹ *DAPNIA, Centre d'Etudes de Saclay, Gif-sur-Yvette, France*

¹⁰ *Department of Physics and Astronomy, University of Glasgow, Glasgow, UK^b*

¹¹ *DESY, Hamburg, Germany^e*

¹² *I. Institut für Experimentalphysik, Universität Hamburg, Hamburg, Germany^f*

¹³ *II. Institut für Experimentalphysik, Universität Dortmund, Dortmund, Germany^a*

¹⁴ *Physikalisches Institut, Universität Heidelberg, Heidelberg, Germany^g*

¹⁵ *Institut für Hochenergiephysik, Universität Heidelberg, Heidelberg, Heidelberg, Germany^g*

¹⁶ *Institut für Reine und Angewandte Kernphysik, Universität Kiel, Kiel, Germany^g*

¹⁷ *Institute of Experimental Physics, Slovak Academy of Sciences, Kosice, Slovakia, Republik*

¹⁸ *School of Physics and Materials, University of Lancaster, Lancaster, UK^b*

¹⁹ *Department of Physics, University of Liverpool, Liverpool, UK^b*

²⁰ *Queen Mary and Westfield College, London, UK^b*

²¹ *Physics Department, University of Lund, Lund, Sweden^b*

²² *Physics Department, University of Manchester, Manchester, UK^b*

²³ *Institute for Theoretical and Experimental Physics, Moscow, Russia*

²⁴ *Lebedev Physical Institute, Moscow, Russia*

²⁵ *Max-Planck-Institut für Physik, München, Germany^g*

²⁶ *LAL, Université de Paris-Sud, IN2P3-CNRS, Orsay, France*

²⁷ *LPNHE, Ecole Polytechnique, IN2P3-CNRS, Palaiseau, France*

²⁸ *LPNHE, Universités Paris VI and VII, IN2P3-CNRS, Paris, France*

²⁹ *Institute of Physics, Czech Academy of Sciences, Prague, Czech Republik*

³⁰ *Nuclear Center, Charles University, Praha, Czech Republic*

³¹ *INFN Roma and Dipartimento di Fisica, Università "La Sapienza", Roma, Italy*

³² *Fachbereich Physik, Bergische Universität Gesamthochschule Wuppertal, Wuppertal, Germany*

³³ *DESY, Institut für Hochenergiephysik, Zeuthen, Germany^g*

³⁴ *Institut für Mittelenergiephysik, ETH, Zürich, Switzerland^g*

³⁵ *Physik-Institut der Universität Zürich, Zürich, Switzerland^g*

³⁶ *Stanford Linear Accelerator Center, Stanford California, USA*

³⁷ *Visitor from Yerevan Phys.Inst., Armenia*

[†] *Deceased*

^a *Supported by the Bundesministerium für Forschung und Technologie, FRG*

^b *Supported by the UK Science and Engineering Research Council*

^c *Supported by IISN-HK/W, NATO CRG-890.78*

^d *Supported in part by USDOE grant DE F603 91ER40674*

^e *Supported by the Swedish Natural Science Research Council*

^f *Supported by the Swiss National Science Foundation*

1 Introduction

The Standard Model of strong and electroweak interactions based on the $SU(3) \otimes SU(2) \otimes U(1)$ gauge group has been successful in describing the phenomenology of high energy particle physics. Nevertheless many fundamental facts, such as the quark-lepton symmetry or the existence of three generations of fermions and their mass spectrum remain unexplained by the model. New states that are not contained in the Standard Model particle spectrum would strongly influence the construction of new theories explaining these facts.

A search for new particles is therefore a priority task at any new accelerator.

The ep collider HERA is an ideal machine to look for leptoquarks and leptogluons that could be produced as s -channel resonances in the electron-parton system. Coloured leptoquark bosons appear naturally in many theories that extend the symmetry of the Standard Model in order to unify the known forces (e.g. grand unified theories [1], superstring inspired models [2]), or models postulating a new interaction (e.g. technicolour [3]), or in some composite models [4]. Leptogluons are predicted in those composite models where the weak gauge bosons and the leptons are bound states of coloured constituents [5]. The search for excited electrons is an obvious field of interest in electron scattering experiments. Excited states of known leptons are a natural ingredient of composite models [6]. If found, they would constitute a strong proof for the existence of a new layer of structure in leptons. HERA provides direct access to a new region of possible values for the masses and coupling constants of these particles.

Although leptoquarks, leptogluons and excited leptons arise in very different theoretical models they have a basic feature in common from a phenomenological point of view. All states discussed in this paper are formed as a resonance between the incoming electron and a constituent of the proton or a gauge boson radiated off the proton. In the narrow width approximation and to lowest order, the ep cross section for the production of a heavy state H decaying into a specific final state with a branching ratio \mathcal{B} is given by:

$$\sigma(ep \rightarrow H + X) = \frac{4\pi^2}{s} (2J+1) \frac{\Gamma}{M} \mathcal{B} f_{i/p}(M^2/s)$$

where J , M are the angular momentum and the mass of H , and \sqrt{s} is the centre of mass energy. The term $f_{i/p}(x)$ denotes for example the quark density functions or the number of photons $f'_{i/p}(x)$ radiated off the proton - as appropriate. The widths Γ and the branching ratios \mathcal{B} contain the dependence on the couplings of the new particles.

In this paper, we present a search for direct single production of new particles based on an integrated luminosity of $\mathcal{L} = 24 \pm 2 \text{ nb}^{-1}$ collected during 1992 at $\sqrt{s} = 296 \text{ GeV}$. Early results from HERA have already been presented [7].

2 Experimental Set-up

A detailed description of the H1 detector can be found elsewhere [8]. Here we briefly describe the components relevant for the present analysis.

The interaction vertices along the z -axis are distributed symmetrically around the centre of the H1 coordinate system ¹ and $\sim 90\%$ of ep events are contained within the

¹The positive z -coordinate (i.e. forward direction) from which θ polar angles are measured is defined to coincide with the direction of the incident proton.

interval $|z_{var}| < 50 \text{ cm}$. The tracks of the emerging charged particles are measured in an array of central and forward drift and proportional chambers covering the angular range $7^\circ \leq \theta \leq 176^\circ$.

The tracking system is surrounded by a finely segmented liquid argon (LAr) sampling calorimeter covering $4^\circ \leq \theta \leq 155^\circ$ with a thickness varying between 20 and 30 radiation lengths for the lead/argon electromagnetic section and from 4.5 up to 8 interaction lengths in total including the stainless-steel/argon hadronic section. A lead/scintillator electromagnetic backward calorimeter extends the coverage at larger angles ($155^\circ \leq \theta \leq 176^\circ$). In the LAr calorimeter, electron energies are measured with a resolution of $\sigma(E)/E \simeq 11\%/\sqrt{E}$ and hadron energies with $\sigma(E)/E \simeq 50\%/\sqrt{E}$ after software energy weighting.

The tracking chambers and calorimeters are surrounded by a superconducting solenoid coil providing a uniform field of 1.2 T parallel to the z -axis within the tracking volume. The return iron yoke surrounding this coil is fully instrumented to measure leakage of hadronic showers and to recognize muons. Muon tracks are measured in layers of streamer tube chambers between $5^\circ \leq \theta \leq 170^\circ$. The system is completed by a forward muon spectrometer in the region $3^\circ \leq \theta \leq 17^\circ$.

The luminosity is determined from the rate of the Bethe-Heitler $ep \rightarrow e\gamma$ process measured in a luminosity monitor as described in [9].

3 Leptoquarks

3.1 Phenomenology

Leptoquarks are colour triplet bosons carrying a fractional electric charge and both leptonic and baryonic quantum numbers. They may couple to electroweak bosons, gluons and electron-quark ($e\bar{q}$) pairs, whereas at accessible masses their coupling to q pairs must vanish to avoid fast proton decay. In ep collisions at HERA, the dominant production mechanism could be by direct resonant eq fusion in the s -channel. This is unlike the situation at other current colliders where the production would be dominated by pair production either via s -channel electroweak gauge boson exchange (in e^+e^- collisions) or via gluon-gluon fusion or $q\bar{q}$ annihilation (in $p\bar{p}$ collisions).

At HERA, besides the dependence on the electric charge, the spin and the weak isospin, leptoquark production also depends on the strength of unknown Yukawa couplings λ to the $e\bar{q}$ pairs. In this paper, we consider the most general effective Lagrangian [10] for baryon and lepton number conserving scalar and vector leptoquark bosons having dimensionless, $SU(3) \otimes SU(2) \otimes U(1)$ invariant couplings to fermions. The isospin families of allowed leptoquarks are given in table 1 where we adopt the nomenclature from [11].

Given the severe low energy experimental constraints on flavour-changing transitions [12], we assume that intergenerational mixing is forbidden and that first generation leptoquarks are only allowed to decay into fermions of the same generation. Moreover, there are limits and precision measurements on branching ratios of pseudoscalar meson decays that constrain most leptoquarks with masses M of $\mathcal{O}(100) \text{ GeV}$ to have sizeable couplings only to either left handed or right handed leptons [12].

which distinguishes them from the $1/y^2$ spectrum yielded by standard vector boson exchange.

Direct searches for scalar leptoquarks have been carried out by e^+e^- collider experiments at PETRA [13, 14], TRISTAN [15] and LEP [16], as well as at $p\bar{p}$ colliders by the UA1 and UA2 experiments at CERN [17] and by CDF at Fermilab's Tevatron [18]. In most cases, the rejection limits were obtained for some scalars with specific quantum numbers. Nevertheless, these limits should only weakly depend on these choices. At 95% confidence level (CL), the LEP experiments exclude the domain $5 \lesssim M_S \lesssim 45$ GeV while UA2 and CDF (preliminary results) exclude $30 \lesssim M_S \lesssim 82$ (113) GeV for a 50% (100%) B into $e + X$, almost independently of the coupling λ .

Finally, it should be noted that an indirect limit of $\lambda_L \lesssim M/1.7$ TeV has been derived [12] from the universality of the Fermi constant measured in μ decays and β decays. Leptoquark exchange with left handed couplings could contribute to the latter. This limit would however be weakened if the Standard Model prediction for the these decays is modified, for instance, by additional Higgs scalars.

Table 1: Isospin multiplets T of scalar (0S_1) and vector (1V_T) leptoquarks with electric charge Q , branching ratio B , and fermion number $F=0$ or $F=1$, and the allowed production and decay channels for first generation leptoquarks at HERA (e^- beam). A coupling value $\lambda_{L(R)} \neq 0$ allows for processes with incident $e^-_{L(R)}$.

$F=2$	T_3	prod.	decay	B	$F=0$	T_3	prod.	decay	B
$-1/3S_0$	0	$e_L^- u_L \rightarrow e^- u$	$1/2$	$-2/3V_6$	0	$e_L^- \bar{d}_R \rightarrow e^- \bar{d}$	$1/2$		
		$\rightarrow \nu_e d$	$1/2$			$\rightarrow \nu_e \bar{u} \bar{d}$	$1/2$		
		$e_R^- u_R \rightarrow e^- u$	1			$e_R^- \bar{d}_L \rightarrow e^- \bar{d}$	1		
$-4/3\tilde{S}_0$	0	$e_L^- d_R \rightarrow e^- d$	1	$-5/3V_6$	0	$e_R^- \bar{u}_L \rightarrow e^- \bar{u}$	1		
		$\rightarrow \nu_e \bar{d}$	$1/2$			$\rightarrow \nu_e \bar{u} \bar{d}$	$1/2$		
$-4/3S_1$	-1	$e_L^- d_L \rightarrow e^- d$	1	$-5/3V_1$	-1	$e_L^- \bar{u}_R \rightarrow e^- \bar{u}$	1		
	0	$e_L^- u_L \rightarrow e^- u$	$1/2$	$-2/3V_1$	0	$e_L^- \bar{d}_R \rightarrow e^- \bar{d}$	$1/2$		
		$\rightarrow \nu_e d$	$1/2$			$\rightarrow \nu_e \bar{u} \bar{d}$	$1/2$		
$+2/3S_1$	1	None		$+1/3V_1$	1	None			
$-4/3V_{1/2}$	-1/2	$e_R^- d_L \rightarrow e^- d$	1	$-5/3S_{1/2}$	$-1/2$	$e_L^- \bar{u}_L \rightarrow e^- \bar{u}$	1		
		$\bar{d}_L \bar{d}_R \rightarrow e^- d$	1			$e_R^- \bar{u}_R \rightarrow e^- \bar{u}$	1		
		$e_R^- u_L \rightarrow e^- u$	1			$e_R^- \bar{d}_R \rightarrow e^- \bar{d}$	1		
$-1/3V_{1/2}$	+1/2			$-2/3S_{1/2}$	$+1/2$				
$-1/3\tilde{V}_{1/2}$	-1/2	$e_L^- u_R \rightarrow e^- u$	1	$-2/3\tilde{S}_{1/2}$	$-1/2$	$e_L^- \bar{d}_L \rightarrow e^- \bar{d}$	1		
	+1/2	None		$+1/3\tilde{S}_{1/2}$	$+1/2$				

3.2 Event Selection and Kinematics

A high transverse energy E_T in the final state is a basic feature for leptoquark events at large masses since E_T^e for $e + X$ decays and E_T^X for $\nu + X$ form a Jacobian peak at $\approx M/2$. In contrast, the background from photoproduction is concentrated at low E_T .

Hence, for $e + X$ final states, a relatively clean sample of candidate events (mostly from high Q^2 neutral current DIS) is obtained by searching for a high E_T electron in the final state. The events are required to have been registered by LAr triggers based on the measured total or transverse energy. All the relevant hardware triggers were simultaneously operational for $\approx 85\%$ of the integrated luminosity. We require that an electron candidate with $E_T > 10$ GeV is found in the fiducial volume of the LAr calorimeter and at $\theta_e > 10^\circ$. The e.m. shower must have at least 90% of its energy deposited in the e.m. section. In addition the shower must be isolated in the sense that there should be less than 10% additional hadronic energy within a cone of azimuthal angle ϕ and pseudorapidity η of opening $\sqrt{(\Delta y)^2 + (\Delta \phi)^2} < 0.5$ centered on the candidate electron and viewed from the interaction vertex. The accepted events are required to have a reconstructed vertex. In events where several ‘electron’ candidates were found, the one with the highest E_T was assumed to originate from the decay (i.e. to be the scattered electron in case of DIS) and was kept for further kinematical analysis. To further reduce contamination from cosmic muon induced showers, we require that there be no track and no energy (> 1 GeV) within the isolation cone in the instrumented iron behind the electron.

The leptoquark mass is calculated using $M = \sqrt{\hat{s}x_e}$. The Bjorken x measured from the final state electron is given by $x_e = E_e E^{lo} \cos^2 \frac{\theta_e}{2} / (E_p^{lo} [E_e^2 - E_p^{lo} \sin^2 \frac{\theta_e}{2}])$, where E_e^2 is the incident electron beam energy (26.7 GeV) and E_p^{lo} is the proton beam energy (820 GeV). The electron energy E_e and the angle θ_e are calculated entirely from energy deposition in the LAr calorimeter viewed from the interaction vertex. The angular resolution thus obtained is of about $\sigma_\theta \simeq 0.7^\circ/\sqrt{E}$ (E in GeV). The method of calculating the mass is well suited to the leptoquark mass reconstruction at large y , our region of interest.

We require a matching between the Bjorken y_e variable measured with the electron and y_h measured via the hadronic flow, $|y_e - y_h| < 0.3$ where

$$y_e = 1 - \frac{E_e - P_{z,e}}{2E_e^0} \quad \text{and} \quad y_h = \frac{E_h - P_{z,h}}{2E_e^0}.$$

Here the subscript h denotes the sum over all particles measured in the LAr calorimeter excluding the electron candidate. Besides removing events where a hard undetected photon was radiated from the initial state electron, the main purpose of this cut is to reject photoproduction events with a misidentified ‘electron’ candidate in the LAr calorimeter and for which the scattered electron usually escapes undetected at low scattering angle in the beam pipe. The remaining event sample was visually scanned and one further cosmic muon event was identified and rejected. Although we impose no explicit matching requirement of the electron shower with an inner central or forward track, all electron candidates of the final sample were accompanied by at least one reconstructed track within the isolation cone. After all selections have been applied, 43 events remain with reconstructed ‘leptoquark’ masses above 35 GeV.

A search for final states with $\nu + X$ is made by requiring a missing transverse momentum of $P_T^{miss} \equiv \sqrt{(\sum E_x)^2 + (\sum E_y)^2} > 20$ GeV measured by the calorimeters. Any event with an electron candidate (as defined above) with $E_T^e > 10$ GeV are rejected. Cosmic muon induced showers were recognized and rejected on the basis of back-to-back tracks in the muon system. Five events with clear cosmic induced patterns were finally rejected at a visual scanning. One event with a $P_T^{miss} \approx 37$ GeV remained, showing the expected signature of a high P_T current jet together with the energy flow from the proton remnant. The leptoquark mass for this event was calculated via the Bjorken x variable computed from the hadronic energy flow, $M = \sqrt{s y_h}$ with

$$x_h = \frac{P_{T,h}^2}{(1 - y_h) y_h s}.$$

The calculated mass of this $\nu + X$ candidate is 93 GeV.

3.3 Results

We first compare our $e + X$ data sample with a Monte Carlo simulation. For the DIS neutral current background, we used the DJANGO event generator [19] which provides an interface to HERACLES [20] for the standard electroweak interactions including first order QED radiative corrections, and LEPTO [21] for QCD corrections (leading log parton showers). The Lund string model is used for fragmentation and decay. The events were passed through the full H1 simulation and reconstruction chain. The trigger efficiencies, monitored by using track triggers, were folded in.

Figure 1 (a) shows the measured P_T^{miss} for the 43 events compared to the DIS event simulation. The events are well balanced in the transverse plane and the DIS Monte Carlo reproduces well the tail of the P_T^{miss} distribution which is due to detector resolution and energy losses. The electron E_T^e extends up to 50 GeV and was found to be very well correlated with the total E_T flow. The electron carries on average about 45% of the total E_T , as one might anticipate for a $e + jet$ final state given the broadening of the jet caused by parton shower and fragmentation effects. The mass distribution is shown in

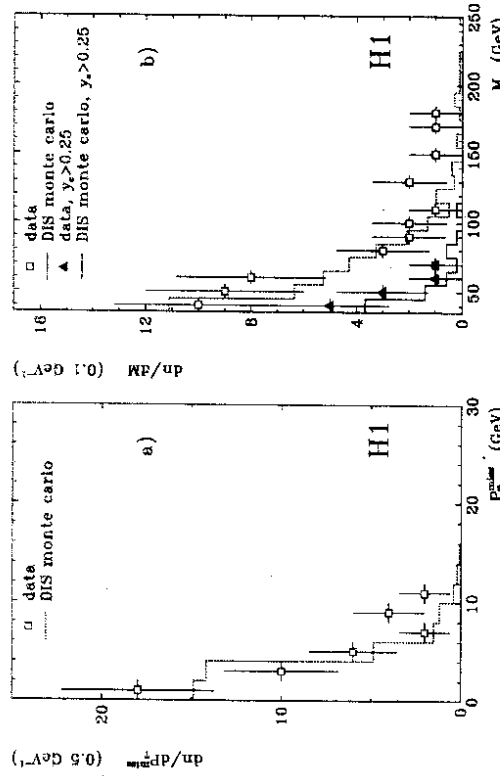


Figure 1: P_T^{miss} distribution (a) and mass spectrum (b) for $M = \sqrt{s_{eS}} > 35$ GeV before (open points) and after (closed points) the final kinematical cut on y_e . The histogram curves show the absolute prediction of a DIS Monte Carlo simulation based on DJANGO before (dashed) and after the (solid) kinematical cut.

fig. 1 (b) before and after a final kinematical cut of $y_e > 0.25$. This cut was chosen as a compromise to optimise the signal-to-background ratio for scalar leptoquark searches while maintaining efficient detection of vector leptoquarks. It also safely rejects the low y region where both y_e and x_h are badly measured. In fig. 1, both the absolute number of events and the shape of the mass spectra are well reproduced by a DIS Monte Carlo simulation before and after the y_e cut.

For $\nu + X$ final states, we apply no additional kinematical cuts compared to those described in section 3.2. Using DJANGO as the basis for event simulation and reconstruction and folding in the LAr trigger efficiencies for the hadronic flow, one predicts a mean number of charged current events of 0.66.

We now derive rejection limits for the hypothesis that all observed events are standard DIS background. To compute efficiencies for the various leptoquark types we make use of the COMPOS event generator [11] which implements the differential cross sections calculated in [10] and which includes radiative corrections in the electron initial state in the collinear approximation. It should be noted that the parton showering (here also generated through the Lund model) is only applied to the final state quark (i.e. after leptoquark decay) and to the ‘diquark’ remnant of the proton. This is despite the fact that for low masses and couplings (e.g. $M_S \lesssim 100$ GeV, $\lambda \lesssim 0.1$), the lifetime of the leptoquark

is such ($\tau \gtrsim 3 \times 10^{-23}$ s) that it must itself participate in the fragmentation before decaying. Such a crude approximation is justified if one considers that leptoquarks may have ‘hard’ fragmentation functions not unlike those of heavy quarks. The mass resolutions $\sigma_{S,V}$ roughly scale with mass at small coupling values (e.g. $\lambda \lesssim 0.3$) for which the intrinsic width of the resonance can be neglected. We find that $\sigma_S = 1.1$ GeV + $9.6 \times 10^{-3} M_S$ for scalars and $\sigma_V = 1.9$ GeV + $9.0 \times 10^{-3} M_V$ for vector leptoquarks in the charged decay mode while in the neutral mode we find $\sigma_S = 4.9$ GeV + $5.7 \times 10^{-2} M_S$ and $\sigma_V = 3.9$ GeV + $4.4 \times 10^{-2} M_V$. The global efficiencies are given in table 2 for both decay modes.

Type \ M (GeV)	50	100	150	200
S e eff. (%)	48	54	50	45
ν eff. (%)	19	52	61	64
V e eff. (%)	30	34	29	21
ν eff. (%)	16	50	61	51
e_8 e eff. (%)	40	44	42	29

Table 2: Detection efficiency within $[M \pm 3\sigma]$ after all selection and kinematical cuts, and including trigger efficiencies for scalar (S) and vector (V) leptoquarks in $e+X$ and $\nu+X$ decay modes as well as for charged leptogluons (e_8).

By moving a mass window of $\pm 3\sigma_{SV}$ around the nominal central value we obtain cross section limits for scalar and vector leptoquarks. In the mass region where we observe no events (e.g. $M \gtrsim 76$ GeV when considering leptoquarks having couplings only to $e+X$ final states), we exclude cross sections for leptoquark production of $\sigma_{ep \rightarrow S,V} \gtrsim 3/(\mathcal{L} \times \epsilon)$ at 95% CL, where ϵ is an efficiency derived from table 2. We exclude, e.g., $\sigma_{ep \rightarrow \tilde{S}_0^R} \gtrsim 247$ pb at 95% CL. From the cross section limits we derive coupling limits for all leptoquarks. Whenever possible, neutral and charged lepton decay modes have been combined. The results in the mass versus coupling constant plane are shown in fig. 2. For couplings of $\lambda = 0.3$ which corresponds to an electromagnetic coupling, i.e. $\alpha = \frac{\lambda^2}{4\pi}$, the mass limits at 95% CL range from 145 GeV to 192 GeV for $F = 2$ and from 98 to 121 GeV for $F = 0$ leptoquarks. The best limits are obtained for the S_1^L , $M \gtrsim 192$ GeV and $V_{1/2}^R$, $M \gtrsim 190$ GeV. For the isosinglet scalars S_0^L and S_0^R which appear in particular in superstring motivated E_6 models [2], we obtain at $\lambda = 0.3$ mass limits of $M \gtrsim 181$ GeV and $M \gtrsim 178$ GeV respectively at 95% CL. We have therefore improved on the current limits from $p\bar{p}$ experiments after only a few months data taking on HERA (for the S_0^L (S_0^R) which has $\mathcal{B} = 50\%$ (100%) into $e+X$, the CDF limit at 95% CL is 82 GeV (113 GeV) almost independently of the coupling λ).

The $\tilde{S}_{1/2}$, for which we find $M \gtrsim 98$ GeV at 95% CL for $\lambda = 0.3$, only couples to $e\bar{d}$ and has been proposed in a recent [22] extension of minimal $SU(5)$. The coupling limits for $\tilde{S}_{1/2}$ may also be interpreted in R-parity violating supersymmetry [23] as limits on the coupling of scalar top squark (stop) provided that a mass eigenstate of the stop exists which is lighter than the top quark and that the total decay width is dominated by R-parity violating decays.

There is an uncertainty on the limits in fig. 2 due to ambiguities in the structure function used in the calculation of leptoquark cross sections. The results presented here have been obtained using the MT-BI parametrisation and were compared with those obtained using MT-B2, MRS-D0 and D- [24]. The differences for the limits on the

coupling constants amount to 7% for leptoquarks coupling to quarks and to 12% for those interacting with anti-quarks. For the QCD scale at which quark densities are evaluated we chose Q^2 . Alternative choices like P_T^2 and M^2 yield an additional uncertainty of 7%.

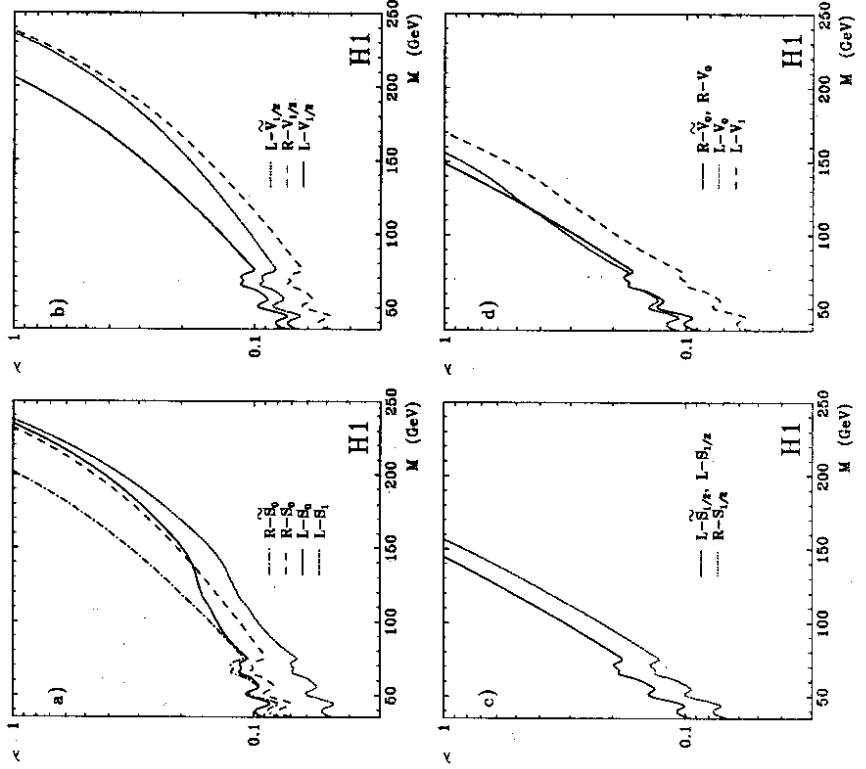


Figure 2: Rejection limits at the 95% CL for the coupling $\lambda_{L,R}$ as a function of mass for scalar and vector leptoquarks with fermion number $F=2$ (a), (b) and $F=0$ (c), (d). The regions above the curves are excluded. The limits on λ_L for S_0, S_1, V_0 and V_1 combine changed and neutral decays.

4 Leptogluons

Leptogluons are colour octet states carrying lepton number which can have dimensionless renormalizable couplings only to gluons. At HERA, we essentially study their coupling to electron-gluon pairs for which an interaction Lagrangian, for a magnetic type coupling,

is given in [25]² where spin 1/2 leptogluons were considered. For such an electron-type leptogluon e_8 , chiral protection must be imposed to avoid the stringent indirect mass limits from $(g-2)_e$ measurements [26] valid for any reasonable scale Λ . We perform the analysis for couplings with left-handed electrons. For the dominant s -channel contribution, the final state angular distribution is independent of this assumption. At HERA, leptogluons would be produced as narrow s -channel resonances through the direct fusion of a lepton and a gluon from the proton. To lowest order, the cross section depends only on the gluon density $g(x, Q^2)$ in the proton at $x = M/\Lambda^2$ and on $(M/\Lambda)^2$, where M is the leptogluon mass and Λ is a scale parameter. The decay width is given by $\Gamma = \alpha_s M^3 / 4\Lambda^2$, where α_s is the strong coupling constant.

Limits on e_8 leptogluons were derived by JADE [14, 25] from the t -channel contribution to the total hadronic cross section, $M_{e_8} \gtrsim (240 \text{ GeV})^3 / \Lambda^2$ and from direct production via one photon exchange, $M_{e_8} \gtrsim 20 \text{ GeV}$. A mass limit of $M > \mathcal{O}(110 \text{ GeV})$ from direct pair production via colour gauge interactions has also been derived from $p\bar{p}$ collider data [27].

The final state of a lepton and a gluon jet (instead of a quark jet) only differs from the one expected for leptoquarks in the details of the jet fragmentation. The analysis presented in the previous section is insensitive to the detailed topology of the hadronic final state. Hence, we make use of the event selection presented there for $e+X$ final states and the corresponding mass distribution presented in fig. 1. We also use COMPOS [11] event generator for this analysis together with the full H1 simulation to estimate leptogluon detection efficiencies after the final $e+X$ kinematical cuts. For leptogluons, the mass resolution σ_{e_8} scales like $\sigma_{e_8} = 0.6 \text{ GeV} + 1.7 \times 10^{-2} M_{e_8}$. These efficiencies are given in table 2 as a function of mass.

Assuming that all the observed events are standard DIS background, we obtain rejection limits at the 95% CL following the procedure described in the previous section. The limits in the Λ^{-1} versus M_{e_8} plane are shown in fig. 3. We exclude at 95% CL scale parameters $\Lambda \lesssim 1.8 \text{ TeV}$ for a leptogluon at $M \simeq 100 \text{ GeV}$ and $\Lambda \lesssim 200 \text{ GeV}$ at $M \simeq 200 \text{ GeV}$.

5 Excited Leptons

5.1 Phenomenology

Strong evidence for a structure of the known fermions would be provided by the direct observation of their excited states. If they exist, such first generation lepton excited states could be produced at HERA in a collision between the incoming electron and a gauge boson radiated from the proton (quark). Excited electrons (e^*) would be generated dominantly via the exchange of low Q^2 photons whereas excited neutrinos (ν^*) would be formed at much higher Q^2 through the interchange of a W gauge boson.

The current maximum available centre of mass energy for the direct production of excited leptons at HERA is 296 GeV. This allows a mass range to be explored for the first time where the decay of the e^* and the ν^* into heavy gauge bosons (W, Z) and a light fermion may become dominant. To date, searches for e^* and ν^* have been pursued using

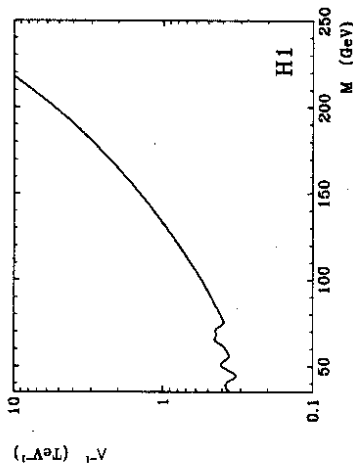


Figure 3: Rejection limits at the 95% CL for the inverse of the scale parameter Λ versus M for e_8 leptogluons. Values above the curve are excluded.

the decay channel with a photon in the final state. The best current rejection limits for the direct single production of excited leptons were obtained by LEP experiments [28, 29, 30, 31] and exclude masses $M_{e^*} \lesssim 90 \text{ GeV}$ almost independently of the composite scale Λ for $\Lambda \lesssim 2.5 \text{ TeV}$.

Although there is no predictive model for composite dynamics, the existence of heavy excited states can still be tested. We make use of an effective $SU(2) \otimes U(1)$ invariant Lagrangian [32] for spin 1/2 excited states. In this model the transition magnetic type couplings of an ordinary lepton (l) and an excited lepton (l^*) to a vector boson (V) with the four momentum q are studied: $-i\frac{\bar{q}}{\Lambda} \sigma_{\mu\nu} q^\nu (1 - \gamma_5) c_{\nu^* l^*}^r$. Here, e is the electric charge and all the coupling constants $c_{\nu^* l^*}$ are explicitly given by

$$\begin{aligned} c_{\gamma^* e^* e} &= -(f + f')/4 \\ c_{\gamma^* \nu^* \nu} &= (f - f')/4 \\ c_{Z^* e^* e} &= -(f \cot \theta_W - f' \tan \theta_W)/4 \\ c_{Z^* \nu^* \nu} &= (f \cot \theta_W + f' \tan \theta_W)/4 \\ c_{W^* \nu^* e} &= c_W e^* \nu = f/(2\sqrt{2} \sin \theta_W) \end{aligned}$$

where θ_W is the weak mixing angle and f and f' are free parameters associated with the gauge groups $SU(2)$ and $U(1)$. The production of the excited leptons depends mainly on the couplings $c_{\gamma^* e^* e}$ and $c_{W^* \nu^* e}$ while for the decay of the excited states the other couplings have to be considered, too. The width Γ introduced in section 1 is given by $\Gamma = \alpha M^3 c_{\nu^* l^*}^2 / \Lambda^2$.

The branching ratios, given in [33, 34] are a priori unknown since they depend crucially on the ratio of the free coupling parameters f and f' . If one sets $f = f' = 1$, the e^* at low masses decays dominantly into a photon and an electron while at higher masses the contribution of the charged weak boson is most significant (see table 3). However, for this

²This Lagrangian has been multiplied by 1/2 to be conform with the more common definition.

choice of the parameters the ν^* can only decay into a W^+ or a Z^0 . For $f = -f' = 1$, the e^* has the photon channel completely suppressed while in this channel the ν^* has its maximal branching ratio. This complementary behaviour together with the arbitrariness of f and f' motivates a search for both the e^* and the ν^* and suggests that as many decay channels as possible should be studied.

M (GeV)	$e^* \rightarrow e\gamma$	$e^* \rightarrow eZ$	$e^* \rightarrow \nu W$	$\nu^* \rightarrow \nu\gamma$	$\nu^* \rightarrow \nu Z$	$\nu^* \rightarrow eW$
100	73 / 0	1 / 14	26 / 86	0 / 73	14 / 1	86 / 26
150	40 / 0	8 / 34	52 / 66	0 / 40	34 / 8	66 / 52
200	34 / 0	10 / 37	56 / 63	0 / 34	37 / 10	63 / 56

Table 3: Branching ratios (in %) of the three decay channels for the excited electron and neutrino. The first number in the columns refers to a setting of $f=f'=1$, the second to $f=-f'=1$.

Therefore, as well as $e^* \rightarrow e^- + \gamma$, the weak boson decay channels also have to be considered for both e^* and ν^* , leading to signatures with electrons, photons or muons in the final state. Table 4 summarizes the decay channels which are studied with the H1 detector. The production and decay of heavy excited leptons considered here, is characterized by one or more energetic e.m. clusters with high E_T in the final state. In addition in some channels a signature with one or two muons and/or missing visible energy should occur.

5.2 Event Selection

The candidate sample for excited leptons was selected by requiring isolated e.m. clusters in the H1 calorimeter. We searched for event topologies with one, two or three such clusters in the final states, and for two muon candidates together with one cluster.

Candidates for events with one-electron or one-photon must have at least one isolated e.m. cluster with more than 15 GeV. The quantity $E_T + P_T^{\text{miss}}$ was required to be greater than 30 GeV and P_T^{miss} should be above 16 GeV. Events with a single cluster in the backward region are excluded to eliminate the DIS ep scattering at low Q^2 . For background suppression, we demand one track in the central drift chambers (with $P_T > 0.2$ GeV) or forward tracking system. The reconstruction efficiency for these tracks is determined from isolated tracks in a DIS data sample with the scattered electron in the LAr calorimeter and from muons crossing the forward chambers. The efficiencies agree with those found in Monte Carlo calculations.

To select candidates for the decay channels with two electrons or with one electron and one photon, two isolated e.m. clusters are demanded with energies above 30 GeV and 15 GeV. At least one cluster has to be in the barrel region ($15^\circ \leq \theta \leq 150^\circ$). No events are expected with both clusters in the forward and backward part of the detector from excited lepton decays.

Candidates for $e^* \rightarrow eee$ are selected requiring three isolated clusters each having an energy above 10 GeV. Here again one cluster should be in the barrel region and only one cluster may be below 10° .

	M (GeV)	$e^* \rightarrow e\gamma$	$e^* \rightarrow eZ$	$e^* \rightarrow \nu W$	$\nu^* \rightarrow \nu\gamma$	$\nu^* \rightarrow \nu Z$	$\nu^* \rightarrow eW$
$e^* \rightarrow e\gamma$					71	82	87
$e^* \rightarrow \nu W / W \rightarrow e\nu$					-	66	67
$e^* \rightarrow eZ / Z \rightarrow ee$					-	72	89
$e^* \rightarrow eZ / Z \rightarrow \mu\mu$					-	47	68
$e^* \rightarrow eZ / Z \rightarrow \nu\nu$					-	-	68
$\nu^* \rightarrow \nu\gamma$					65	73	79
$\nu^* \rightarrow eW / W \rightarrow e\nu$					-	63	75
$\nu^* \rightarrow eW / W \rightarrow \mu\nu$					-	25	62
$\nu^* \rightarrow \nu Z / Z \rightarrow ee$					-	75	81

Table 4: Total efficiencies (in %) for different decay channels and masses of the excited leptons e^* and ν^* .

In summary, after applying selection criteria which are motivated by Monte Carlo studies, no candidates are left in any of the channels under study.

5.3 Results

With a typical efficiency of 80 %, cross sections above 160 pb are ruled out with 95% CL for each channel under study. This result depends only weakly on the used model.

We have calculated coupling limits as a function of the parameter $c_{\nu^* \nu}$, the scale parameter Λ and the square root of the branching ratios of the excited leptons introduced in section 5.1. These limits are shown in fig. 4 for different decay channels (see table 4) as a function of the mass of the excited lepton.

In principle, coupling limits can be calculated up to the maximum of the centre of mass energy of the collisions for the direct search of excited leptons. But the calculations are limited in this analysis to masses and coupling values where the decay width is below 30 GeV. This ensures that the width is always much less than the corresponding mass. For $f = 0, f' = 1$ this width is reached at $M = 215$ GeV for the excited electron and at 165 GeV for the excited neutrino. If it should happen in nature that $f = f' = 1$ then the width of 30 GeV would be obtained at 175 GeV for the e^* , whereas if $f = 1, f' = -1$ should be true, then limits for the ν^* can only be derived up to 125 GeV.

The dominant uncertainty on these limits is due to the possible choice of the different proton structure functions. Using the same functions as in section 3.3 we obtain uncertainties on the limits up to 10%.

6 Conclusions

We have searched with the H1 detector for direct production of scalar and vector leptoquarks, leptogluons, excited electrons (e^*) and excited neutrinos (ν^*) in a mass range extending up to ~ 250 GeV. This mass range is not accessible directly at other existing colliders.

Scalar and vector leptoquarks of all possible $SU(2) \otimes U(1)$ multiplet assignments were searched for. No evidence was found for the production of such states and coupling limits were calculated as a function of mass. For a coupling value of $\lambda = 0.3$ we obtain mass limits at 95% CL ranging from $M \gtrsim 145$ GeV to $M \gtrsim 192$ GeV for leptoquarks resulting from the fusion of an electron and a quark and from 98 to 121 GeV for leptoquarks formed with an antiquark. We obtain, e.g., $M > 192$ GeV for S_L^L and $M > 190$ GeV for $V_{1/2}^R$ at 95% CL. Finally we found no evidence for lepto gluons and at 95% CL exclude the scale region $\Lambda \lesssim 1.8$ TeV for $M \simeq 100$ GeV.

The analysis of the e^* and ν^* included an investigation of several decay topologies. This search for channels with electroweak bosons in the final state is possible owing to the available centre of mass energy and is necessary because depending on the models some channels are suppressed while others are enhanced. No evidence was found for the production of e^* or ν^* . Cross sections above 160 pb are ruled out with 95% CL for a detection efficiency of 80%. For this direct search, limits on couplings have been presented in a new accessible mass domain.

7 Acknowledgements

We are very grateful to the HERA machine group whose outstanding efforts made this experiment possible. We wish to acknowledge the support of the DESY technical staff. We appreciate the many contributions of our engineers and technicians who constructed and maintained the detector. We thank the funding agencies for financial support of this experiment. The non-DESY members of the collaboration also wish to thank the DESY directorate for the hospitality extended to them.

References

- [1] J.C. Pati and A. Salam, Phys. Rev. D10 (1974) 275; P. Langacker, Phys. Rep. 72 (1981) 185; G. Senjanović and A. Šokorac, Z. Phys. C20 (1983) 255; H. Georgi and S.L. Glashow, Phys. Rev. Lett. 32 (1974) 438.

At 100 GeV the value for $c_{\nu^* \nu} \sqrt{B}/\Lambda$ is 7×10^{-3} GeV $^{-1}$. Values at LEP experiments at a centre of mass energy of 90 GeV for $c_{\nu^* \nu} \sqrt{B}/\Lambda$ are about 2×10^{-4} GeV $^{-1}$ for the channel $e^* \rightarrow e\gamma$. In order to reach this magnitude for a mass of 100 GeV at HERA, an integrated luminosity of $O(50$ pb $^{-1})$ has to be collected. In the scattering process $e^+ e^- \rightarrow \gamma\gamma$ indirect limits for $c_{\nu^* \nu} \sqrt{B}/\Lambda$ exist [28, 29, 30], and are in the order of 10^{-2} GeV $^{-1}$ up to masses of 127 GeV.

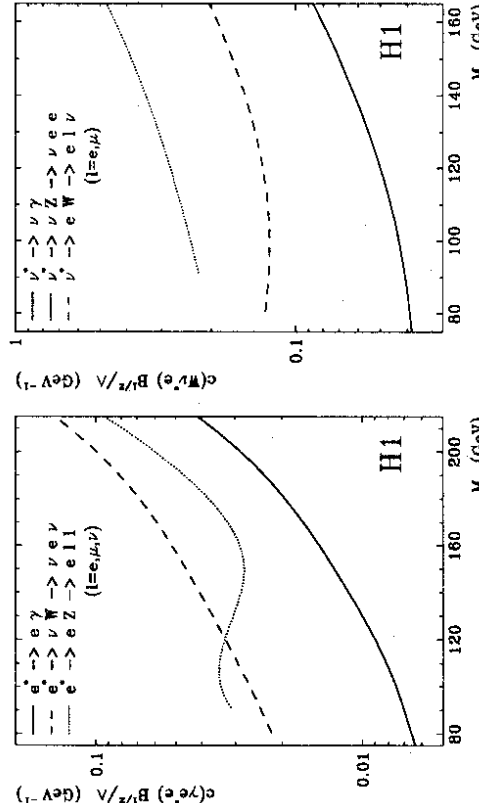


Figure 4: Rejection limits with a CL of 95% for the e^* and the ν^* . Regions above the curves are excluded. For masses above 120 GeV the main contribution in the decay channel $e^* \rightarrow eZ$ stems from the decay $Z \rightarrow \nu\nu$. For lower masses the trigger efficiency for this channel decreases and in that region the limits are determined by the decays $Z \rightarrow e^+ e^- (\mu^+ \mu^-)$.

- [2] A. Dobado, M.J. Herrero and C. Muñoz, Phys. Lett. B191 (1987) 447; V.D. An gelopoulos et al., Nucl. Phys. B292 (1987) 59; J.F. Gunion and E. Ma, Phys. Lett. B195 (1987) 257; R.W. Robinett, Phys. Rev. D37 (1988) 1321; J.A. Grifols and S. Peris, Phys. Lett. B201 (1988) 287.
- [3] S. Dimopoulos and L. Susskind, Nucl. Phys. B155 (1979) 237; S. Dimopoulos, Nucl. Phys. B168 (1980) 69; E. Farhi and L. Susskind, Phys. Rev. D20 (1979) 3404; Idem, Phys. Rep. 74 (1981) 277.
- [4] B. Schrempp and F. Schrempp, Phys. Lett. B153 (1985) 101, and references therein;
- J. Wudka, Phys. Lett. B167 (1986) 337.
- [5] H. Fritzsch and G. Mandelbaum, Phys. Lett. B102 (1981) 319; U. Baur and K.H. Streng, Z. Phys. C30 (1986) 325.
- [6] See for instance
M.E. Peskin, Proc. of the Xth Symposium on Lepton-Photon Interactions, editor
W. Peil, Bonn (1981) p 880.
- [7] F. Eisele, H1 Collaboration, Proc. of the XXVith Int. Conf. on High Energy Physics, Dallas (August 1992); and DESY preprint 92-140 (October 1992); B. Loehr, ZEUS Collaboration, Proc. of the XXVith Int. Conf. on High Energy Physics, Dallas (August 1992); M. Derrick et al., ZEUS Collaboration, DESY 93-017.
- [8] F.W. Brasse, H1 Collaboration, Proc. of the XXVith Int. Conf. on High Energy Physics, Dallas (August 1992); and DESY preprint 92-140 (October 1992); G. Cozzika, H1 Collaboration, 3rd Int. Conf. on Calorimetry in High Energy Physics, Corpus Christi, Texas.
- [9] T. Ahmed et al., H1 Collaboration, Phys. Lett. B299 (1993) 374.
- [10] W. Buchmüller, R. Rückl and D. Wyler, Phys. Lett. B191 (1987) 442.
- [11] T. Köhler, Proc. of the Workshop Physics at HERA, DESY, Hamburg (October 1991) Vol. 3 p 1526 (COMPOS version 1.4).
- [12] W. Buchmüller and D. Wyler, Phys. Lett. B177 (1986) 377; O. Shanker, Nucl. Phys. B204 (1982) 375; Ibid, Nucl. Phys. B206 (1982) 253.
- [13] H.-J. Behrend et al., CELLO Collaboration, Phys. Lett. B178 (1986) 452.
- [14] W. Bartel et al., JADE Collaboration, Z. Phys. C36 (1987) 15.
- [15] G.N. Kim et al., AMY Collaboration, Phys. Lett. B240 (1990) 243; A. Miyamoto, Proc. of the XXVth Rencontre de Moriond, Les Arcs, France, (March 1990).
- [16] D. Decamp et al., ALEPH Collaboration, Phys. Rep. 216 (1992) 253; P. Abreu et al., DELPHI Collaboration, Phys. Lett. B275 (1992) 222; B. Adeva et al., L3 Collaboration, Phys. Lett. B261 (1991) 169; G. Alexander et al., OPAL Collaboration, Phys. Lett. B263 (1991) 123.
- [17] S. Geer, UA1 Collaboration, Proc. of the Europhys. Conf. on High Energy Physics, Uppsala, Sweden, (July 1987); H. Grassman, Ph.D. thesis, RWTH Aachen (1988); J. Alliti et al., UA2 Collaboration, Phys. Lett. B274 (1992) 507.
- [18] M.S. Gold, CDF Collaboration, to be published in the Proc. of the 26th International Conference on High Energy Physics (ICHEP92), Dallas, USA (August 1992), Fermilab preprint CONF-92-287-E; S.M. Moulding, CDF Collaboration, to be published in the Proc. of the Seventh Meeting of the American Physical Society (DPF), Fermilab, USA (November 1992), Fermilab preprint CONF-92-341-E.
- [19] G.S. Schuler and H. Spiesberger, Proc. of the Workshop Physics at HERA, DESY, Hamburg (October 1991) Vol. 3 p 1419 (DJANGO version 1.0).
- [20] A. Kwiatkowski, H. Spiesberger and H.-J. Möhring, Comp. Phys. Commun. 66 (1992) 155 and references therein (HERACLES version 3.1).
- [21] G. Ingelman, (LEPTO version 5.2), program manual unpublished; H. Bengtsson, G. Ingelman and T. Sjöstrand, Nucl. Phys. B301 (1988) 554.
- [22] H. Murayama and T. Yanagida, Tohoku U. preprint TU-370 (May 1991).
- [23] T. Kon and T. Kobayashi, Phys. Lett. B270 (1991) 81.
- [24] A.D. Martin, W.J. Stirling and R.G. Roberts, Durham preprint, DTP-92-16 (1992); J. Morfin and W.K. Tung, Z. Phys. C52 (1991) 13.
- [25] J. Bijnens, Proc. of the 1987 HERA Workshop, DESY, Hamburg (October 1987) Vol. 2 p 819.
- [26] U. Baur and K.H. Streng, Z. Phys. C30 (1986) 325; K.H. Streng, Z. Phys. C33 (1986) 247.
- [27] U. Baur and K.H. Streng, Phys. Lett. B162 (1985) 387.
- [28] D. Decamp et al., ALEPH Collaboration, Phys. Rep. 216 (1992) 253.
- [29] O. Adriani et al., L3 Collaboration, Phys. Lett. B288 (1992) 404; B. Adeva et al., L3 Collaboration, Phys. Lett. B252 (1990) 525.
- [30] M.Z. Akrawy et al., OPAL Collaboration, Phys. Lett. B257 (1991) 531; Idem, Phys. Lett. B244 (1990) 135.
- [31] P. Abreu et al., DELPHI Collaboration, Z. Phys. C53 (1992) 41; Idem, Phys. Lett. B268 (1991) 296.
- [32] K. Hagiwara, S. Komamiya and D. Zeppenfeld, Z. Phys. C29 (1985) 115.
- [33] F. Boudjema, A. Djouadi and J.L. Kneur, DESY preprint 92-116, Hamburg (August 1992) and preprint ENSLAPP-A-385/92.
- [34] J. Kühn and P. Zerwas, Phys. Lett. B147 (1984) 189.
- [35] F. Raupach, Proc. of the Workshop Physics at HERA, DESY, Hamburg (October 1991) Vol. 3 p 1473; A. Courau and P. Kessler, Phys. Rev. D46 (1992) 117.